ORIGINAL ARTICLE

Nonrapid eye movement sleep electroencephalographic oscillations in idiopathic rapid eye movement sleep behavior disorder: a study of sleep spindles and slow oscillations

Jun-Sang Sunwoo[1,†,], Kwang Su Cha[2,†,], Jung-Ick Byun[3], Jin-Sun Jun[4], Tae-Joon Kim[5], Jung-Won Shin[6], Soon-Tae Lee[2], Keun-Hwa Jung[2], Kyung-Il Park[7], Kon Chu[2], Manho Kim[2,8], Sang Kun Lee[2,9], Han-Joon Kim[2], Carlos H. Schenck[10] and Ki-Young Jung[2,9,*,]

[1]Department of Neurosurgery, Seoul National University Hospital, Seoul, South Korea, [2]Department of Neurology, Seoul National University Hospital, Seoul, South Korea, [3]Department of Neurology, Kyung Hee University Hospital at Gangdong, Kyung Hee University College of Medicine, Seoul, South Korea, [4]Department of Neurology, Kangnam Sacred Heart Hospital, Hallym University College of Medicine, Seoul, South Korea, [5]Department of Neurology, Ajou University School of Medicine, Suwon, South Korea, [6]Department of Neurology, CHA Bundang Medical Center, CHA University, Seongnam, South Korea, [7]Department of Neurology, Seoul National University Hospital Healthcare System Gangnam Center, Seoul, South Korea, [8]Protein Metabolism and Dementia Research Center, Seoul National University College of Medicine, Seoul, South Korea, [9]Neuroscience Research Institute, Seoul National University College of Medicine, Seoul, South Korea and [10]Minnesota Regional Sleep Disorders Center and Department of Psychiatry, Hennepin County Medical Center, University of Minnesota Medical School, Minneapolis, MN

†These authors contributed equally to this work.

*Corresponding author. Ki-Young Jung, Department of Neurology, Seoul National University Hospital, Seoul National University College of Medicine, 101 Daehak-ro, Jongno-gu, Seoul, 03080, South Korea. Email: jungky@snu.ac.kr.

Abstract

Study Objectives: We investigated electroencephalographic (EEG) slow oscillations (SOs), sleep spindles (SSs), and their temporal coordination during nonrapid eye movement (NREM) sleep in patients with idiopathic rapid eye movement (REM) sleep behavior disorder (iRBD).

Methods: We analyzed 16 patients with video-polysomnography-confirmed iRBD (age, 65.4 ± 6.6 years; male, 87.5%) and 10 controls (age, 62.3 ± 7.5 years; male, 70%). SSs and SOs were automatically detected during stage N2 and N3. We analyzed their characteristics, including density, frequency, duration, and amplitude. We additionally identified SO-locked spindles and examined their phase distribution and phase locking with the corresponding SO. For inter-group comparisons, we used the independent samples t-test or Wilcoxon rank-sum test, as appropriate.

Results: The SOs of iRBD patients had significantly lower amplitude, longer duration ($p = 0.005$ for both), and shallower slope ($p < 0.001$) than those of controls. The SS power of iRBD patients was significantly lower than that of controls ($p = 0.002$), although spindle density did not differ significantly. Furthermore, SO-locked spindles of iRBD patients prematurely occurred during the down-to-up-state transition of SOs, whereas those of controls occurred at the up-state peak of SOs ($p = 0.009$). The phase of SO-locked spindles showed a positive correlation with delayed recall subscores ($p = 0.005$) but not with tonic or phasic electromyography activity during REM sleep.

Conclusions: In this study, we found abnormal EEG oscillations during NREM sleep in patients with iRBD. The impaired temporal coupling between SOs and SSs may reflect early neurodegenerative changes in iRBD.

Statement of Significance

Electroencephalographic (EEG) slowing during both wakefulness and rapid eye movement (REM) sleep has been reported in patients with idiopathic REM sleep behavior disorder (iRBD), little evidence exists regarding EEG abnormalities during nonrapid eye movement (NREM) sleep. In this study, we found significant alterations in slow oscillation (SO) and sleep spindle (SS) activities during NREM sleep in patients with iRBD. Moreover, the phase of SO-locked SSs was significantly advanced in patients with iRBD compared with that in controls, which was correlated with memory decline. The impaired SO–SS temporal coupling in iRBD may reflect early neurodegenerative changes involving the thalamo-cortical networks.

Key words: NREM sleep; sleep spindle; slow oscillation; REM sleep behavior disorder

Introduction

Sleep consists of two distinct states: nonrapid eye movement (NREM) sleep and rapid eye movement–(REM) sleep. They have distinct patterns of brain activity, which are seen as distinct electroencephalography (EEG) oscillations. NREM sleep-specific EEG rhythms include slow oscillations (SOs) and sleep spindles (SSs) [1]. SO refers to EEG activity <1 Hz reflecting rhythmic alterations in membrane potentials of cortical neurons between depolarized up-states and hyperpolarized down-states [2]. SSs are waxing-and-waning 11–15 Hz oscillations predominantly in the central and parietal brain regions. They are generated in the thalamus and synchronized at the cortical level, reflecting a fundamental efficiency of the thalamo-cortical system [3]. A decrease in SS activity has been implicated in various neurological disorders, including Alzheimer's disease, Parkinson's disease (PD), and schizophrenia [4–6]. Moreover, in healthy adults, a reduction in fast spindles in the frontal region was associated with age-related memory deficits [7]. It has been established that SSs are grouped by SOs during NREM sleep; spindle activity increases during up-states and decreases during down-states of SOs [8]. Moreover, synchronization between SOs and SSs in the thalamo-cortical circuits are crucial for sleep-dependent memory consolidation [9].

REM sleep behavior disorder (RBD) is a parasomnia characterized by abnormal motor behavior and unpleasant dreams during REM sleep [10]. It is commonly associated with α-synucleinopathy neurodegeneration, such as PD and dementia with Lewy bodies (DLB). Idiopathic or isolated rapid eye movement (REM) sleep behavior disorder (iRBD) refers to RBD in the absence of any associated neurological diseases and precipitating factors, such as antidepressant medication use [11]. It is noteworthy that iRBD is the most powerful predictor of the future development of overt neurodegenerative diseases [12]. As a prodromal stage of α-synucleinopathy, neurodegenerative markers, such as olfactory and autonomic dysfunction, subtle motor phenomena, and cognitive impairment, are commonly found in patients with iRBD [13]. Additionally, previous EEG and neuroimaging studies have shown that the disease process of iRBD is not confined to the brainstem REM sleep-generating neurons, but involves widespread cortical and subcortical structures [14–17].

It has been reported that iRBD patients have lower SS density than controls [18, 19]. Higher power of sleep slow waves was associated with a slower progression of axial motor symptoms in PD [20]. Characterizing SOs can provide useful information about excitability, connectivity, and local network activity of the cerebral cortex [21]. Moreover, precise temporal coupling between SO and SS suggests the integrity of cortico-thalamic network underlying memory consolidation during sleep [1]. Although a major pathologic mechanism of iRBD is neurodegeneration of brainstem neurons responsible for generating REM sleep atonia, cortical changes and cognitive deficits frequently found in patients with iRBD suggest the possibility of abnormal cortico-subcortical networks and altered coordination between SO and SS during NREM sleep [16]. However, the SO activity and coordination between SOs and SSs in iRBD have not yet been studied. Therefore, we herein evaluated SO and SS activities and their temporal coordination during NREM sleep in patients with iRBD.

Methods

Participants

We prospectively recruited 25 drug-naïve patients with iRBD and 16 age- and sex-matched controls from October 2014 to May 2019 at the Department of Neurology of the Seoul National University Hospital. RBD was confirmed using video-polysomnography (vPSG) according to the third edition of the International Classification of Sleep Disorders (ICSD-3) [22]. All participants underwent neurological examination and cognitive tests to rule out associated neurodegenerative diseases, such as PD and DLB. They completed questionnaires such as the Korean version of RBD questionnaire-Hong Kong (RBDQ-KR), Epworth sleepiness scale (ESS), and Pittsburgh sleep quality index (PSQI). For neurodegenerative risk markers, we administered scales for outcomes in PD for autonomic symptoms (SCOPA-AUT), the Korean version of Sniffin' Sticks (KVSS), and the Korean version of the Geriatric Depression Scale (GDS-K). Neurocognitive tests included the Korean version of the Montreal Cognitive Assessment (MoCA-K) and the Mini-Mental State Examination (MMSE). Healthy controls were recruited by advertisement, and those with sleep complaints or a history of neurological, psychiatric, or sleep disorders were excluded. For both iRBD and control groups, those with moderate-to-severe obstructive sleep apnea (apnea–hypopnea index > 15 events/h) were excluded from the analysis. This study protocol was approved by the institutional review board of Seoul National University Hospital (No. 1406100589) and conducted in accordance with the Declaration of Helsinki. All participants provided written informed consent before taking part in this study.

Video-polysomnography

All participants underwent single-night in-lab vPSG recordings (Natus, Pleasanton, CA, USA). The recording system is composed of 21-channel EEG, two-channel electrooculography, electromyography (EMG) of the submentalis and tibialis anterior muscles, and electrocardiography. EEG electrodes were placed according to the international 10–20 system. EEG data were recorded using a linked-mastoid reference and a sampling rate of 500 Hz. Respiratory monitoring was conducted using a thermal airflow sensor, nasal pressure transducer, finger pulse oximeter, and thoraco-abdominal piezoelectric belts. A body position sensor and snore sensor were also employed. The time-synchronized video and audio recordings were used to detect abnormal motor behaviors during sleep. Sleep stages and associated events were scored in 30-s epochs according to the American Academy of Sleep Medicine (AASM) manual [23]. The visual scoring of REM sleep without atonia (RSWA) was performed according to the AASM manual criteria with some modifications [23]. Tonic and phasic EMG activity were measured only in the submentalis muscle [24]. Tonic EMG activity was defined as a 30-s REM sleep epoch with at least 50% of the duration of the epoch having an EMG amplitude greater than two times the background EMG activity. Phasic EMG activity was defined as a 30-s REM sleep epoch with at least five 3-s mini-epochs containing bursts of transient submentalis muscle activity. Transient muscle activity bursts had to be 0.1–5.0 s in duration and at least four times as high in amplitude as was the background EMG activity.

EEG preprocessing and spectral analyses

All EEG analyses were performed using MATLAB 2017b (MathWorks, Natick, MA). Bandpass filtering with zero phase shift was performed to the whole EEG data in the range of 0.3–70 Hz to reduce background noise. EEG data were then segmented into 30-s epochs. Individual epochs were rejected when the EEG voltage exceeded the range of –300 to 300 μV. To observe spectral characteristics during NREM, the power spectra of each 30-s epoch were calculated using Welch's method with NFFT = 512, a 50% overlapping window, and 5-s window segments. The power spectra were averaged over all epochs. The relative power spectral density was computed as a ratio of the absolute power of each frequency band to the total power from 0.3 to 30 Hz. The frequency bands were defined as follows: delta (0.3–4 Hz), theta (4–8 Hz), alpha (8–12 Hz), and beta (12–30 Hz).

SS and SO detection and analyses

SSs and SOs were detected based on previously established detection algorithms [25]. The algorithm to extract SSs and SOs was applied to EEG during stage N2 and N3 sleep. The SS and SO detection methods have been described elsewhere [26]. Briefly, EEG data were low-pass filtered at 35 Hz by applying a Hamming window-based finite impulse response (FIR) filter and down-sampled to 100 Hz. The individual peak frequency in the range of 10–16 Hz was determined based on the power spectra. The EEG signals were then filtered with a ±1.5 Hz bandwidth centered on the individual peak frequency. The root mean square (RMS) value of the filtered EEG signals was computed using a 0.2-s sliding window with a 10-ms step size. Additional smoothing was performed with the same sliding window average of 0.2 s. Moving RMS signals exceeding a threshold of 1.5 standard deviations of the filtered signal with a minimum and maximum duration of 0.5 and 3 s, respectively, were considered as spindle intervals. We investigated SS characteristics including density (number of spindles per min), duration, amplitude (potential difference between the maximum trough and peak), and average frequency observed in the central brain regions (C3, Cz, and C4).

We then identified the spectral characteristics of SSs by constructing a time-frequency map. A time-frequency map for each single spindle was computed using a continuous wavelet transform (CWT) with the complex Morlet wavelet as a mother wavelet function. The time-frequency maps of all spindle events were averaged at each electrode. SS power was determined in the frequency range of 12–16 Hz and time interval of –400 to 400 ms centered on the peak of the spindle envelope. We then calculated the average spindle power at each electrode for each subject.

For SO detection, we applied a 0.3-Hz high-pass filter using a Butterworth window-based infinite impulse response filter and a 3.5-Hz low-pass filter using a Hamming window-based FIR filter. All consecutive positive-to-negative zero crossings corresponding to a time interval range of 0.8–2.0 s duration were marked as putative SOs. Putative SOs were further chosen if their amplitudes were larger than 1.25 times the average amplitude of the subject. An individually adjusted amplitude threshold was used for SO detection because using a fixed amplitude threshold underestimates SO density in older adults and possibly more in iRBD patients [27]. The SO duration was defined as an interval between two consecutive down-zero crossings. The SO frequency was measured by an inverse of twice the down-to-up-peak time interval. The SO amplitude was calculated as the absolute difference in potential between up-peak and down-peak. We determined the above SO characteristics along with density (number of SOs per min) and maximum slope (between down-peak and up-peak) in the frontal regions (F3, Fz, and F4).

Relationship between SO and spindle activity

We examined the spectral characteristics of spindle activity that was observed around the up-peak of SOs to investigate the temporal relationships between spindles and SOs. We selectively analyzed spindle-specific SOs by extracting the SOs that co-occurred with spindles during the up-state of SOs. By applying CWT, we represented the time-frequency map of each single SO event in a time window of –0.5 to 2.0 s around the down-zero crossing of SOs. Normalization was adopted for each frequency of the baseline period (–2.0 to –1.5 s). SO events that had another SO event within ± 4 s were excluded from the analysis to avoid distortion of the baseline period. The time-frequency maps were obtained by averaging the time-frequency maps of SO events of individual subjects. The SO-locked spindle power was defined as the local maximum power within the frequency range of 12–16 Hz and time range of 500–1,000 ms after the SO onset. For inter-group comparison, the SO-locked spindle power was averaged over nine mid-line electrodes (F3, Fz, F4, C3, Cz, C4, P3, Pz, and P4).

We examined the temporal distribution of SO-locked SS activity. We quantified the degree of phase locking between SSs and SOs by calculating the phase locking value (PLV) of SO-locked SSs for each subject [28]. We extracted the phase of the SS that peaked during the SO up-state. The phase of the spindle peak was computed based on the duration of the SO up-state. PLV was calculated as follows:

$$PLV = \frac{\left| \sum_{n=1}^{N} e^{i(\theta_{SP_n} - \theta_{SO_n})} \right|}{N},$$

where N is the total number of detected SOs, θ_{SP_n} is the phase of the spindle peak within the SO up-state, and θ_{SO_n} is the phase of the SO up-peak. The PLV and phase of SO-locked SSs were compared between groups.

Statistical analyses

The assumption of normality of continuous variables was tested using the Kolmogorov–Smirnov test. Clinical and PSG data were not normally distributed and compared using the Wilcoxon rank-sum test. Power spectrum and SO and SS activity data were normally distributed, and an independent samples t-test was used for inter-group comparisons. Multiple comparisons of the scalp topography between the iRBD and control groups were corrected using the false discovery rate approach. Comparisons for other variables, including clinical and vPSG parameters, power spectral density, SO and SS characteristics, and SO-locked spindle measures, were corrected with the Bonferroni method. To control for the effect of age and other clinical variables, we additionally performed analysis of covariance for SO and SS characteristics, and SO-locked spindle measures with age or clinical variables as a covariate. Effect size was measured by partial eta squared. As the original data for SS power violated

the assumption of homogeneity of variances, we applied logarithmic transformation to this data and performed analysis of covariance. Correlation analysis was performed using the Pearson correlation coefficient, which was also corrected with the Bonferroni method. The criterion for statistical significance was a two-tailed probability value of $p < 0.05$. All statistical analyses were carried out using SPSS software (version 25, IBM Corp., Armonk, NY).

Results

Clinical and polysomnographic findings

Among the recruited participants, nine patients with iRBD and six controls were excluded because they were found to have moderate-to-severe obstructive sleep apnea. We then analyzed 16 patients with iRBD (age, 65.4 ± 6.6 years; male, 87.5%) and 10 controls (age, 62.3 ± 7.5 years; male, 70%). The mean duration of RBD symptoms was 3.7 ± 2.0 years, and the mean RBDQ-KR score was 50.2 ± 19.6. Regarding prodromal clinical markers, patients with iRBD showed lower KVSS scores than those of controls, but the difference was not significant after multiple testing correction. There was also no significant difference in MMSE, MoCA-K, ESS, SCOPA-AUT, or GDS-K scores (Table 1). For RSWA, tonic and phasic EMG activities of patients with iRBD were 39.7 ± 21.0% and 11.9 ± 10.3%, respectively, which was significantly higher than those of controls (4.1 ± 3.6% and 1.4 ± 1.4%; $p < 0.001$ and 0.001, respectively). Mild obstructive sleep apnea was found in 62.5% of iRBD patients and 80% of controls ($p = 0.420$). The mean apnea–hypopnea index of the controls tended to be higher than that of the iRBD patients (10.2 ± 3.9 vs. 6.1 ± 3.5/h), which did not reach statistical significance after the Bonferroni correction. Other PSG-measured sleep parameters, such as total sleep time, sleep efficiency, and REM latency and percentage, did not differ between the two groups (Table 2).

Table 1. Clinical characteristics of the study participants

Variables	iRBD ($n = 16$)	Control ($n = 10$)	p
Age, years	65.4 ± 6.6	62.3 ± 7.5	0.262
Sex, male	14 (87.5%)	7 (70.0%)	0.340
BMI, kg/m²	23.7 ± 2.8	24.6 ± 2.0	0.391
Education, years	12.8 ± 3.5	12.0 ± 3.4	0.586
Symptom duration, years	3.7 ± 2.0		
RBDQ-KR	50.2 ± 19.6	6.1 ± 4.8	<0.001*
Factor 1	14.9 ± 7.0	3.5 ± 2.8	<0.001*
Factor 2	35.3 ± 14.6	2.6 ± 3.0	<0.001*
MoCA-K	25.6 ± 3.3	27.9 ± 1.8	0.077
MMSE	27.9 ± 2.4	29.0 ± 1.3	0.241
ESS	5.3 ± 2.8	4.0 ± 1.4	0.201
PSQI	4.4 ± 1.7	3.9 ± 1.9	0.623
KVSS	4.6 ± 1.2	5.9 ± 0.9	0.020
SCOPA-AUT	10.9 ± 5.2	7.7 ± 4.2	0.109
GDS-K	11.4 ± 5.5	8.1 ± 8.8	0.201

Data are mean ± standard deviation or number (%). Wilcoxon rank-sum tests were used compare the two groups. iRBD, idiopathic REM sleep behavior disorder; BMI, body mass index; RBDQ-KR, Korean version of RBD questionnaire—Hong Kong; MoCA-K, Korean version of Montreal cognitive assessment; ESS, Epworth sleepiness scale; PSQI, Pittsburgh sleep quality index; KVSS, Korean version of Sniffin' sticks; SCOPA-AUT, scales for outcomes in PD for autonomic symptoms; GDS-K, Korean version of the Geriatric Depression Scale.
*Significant after the Bonferroni correction ($\alpha = 0.05/14$).

Spectral power during NREM sleep

Patients with iRBD showed decreased alpha-band power during NREM sleep compared with that in controls, but the difference did not survive the Bonferroni correction. There was also no difference in delta-, theta-, or beta-band power between the two groups (Figure 1, A). In the scalp topography, the decrease in alpha-power in iRBD patients was significant in most brain regions (Figure 1, B). Although the delta power of iRBD patients tended to be lower than that of controls, the difference was not statistically significant.

SO analysis

Patients with iRBD showed decreased SO amplitude (96.8 ± 13.8 vs. 118.9 ± 22.6 μV, $p = 0.005$) and increased SO duration (1.33 ± 0.07 vs. 1.25 ± 0.07 s, $p = 0.005$) compared with those of controls (Figure 2, A and Table 3). However, SO density did not differ between the two groups (2.4 ± 0.9 vs. 2.9 ± 0.6/min, $p = 0.157$). We further compared the characteristics of the SO waveform. The SOs of iRBD patients were characterized by a shallower maximal slope between down- and up-states (414.2 ± 51.6 vs. 535.7 ± 94.8 μV/s, $p < 0.001$) and delayed up-state peak latency (954.8 ± 61.8 vs. 865.4 ± 66.0 ms, $p = 0.002$) in comparison with those of controls (Figure 2, B). Among the SO characteristics, the most significant difference between the two groups was the decreased maximum slope, which remained significant after adjusting for age, apnea–hypopnea index, or other clinical variables (Supplementary Table S1).

SS analysis

There was no significant difference in SS amplitude (20.8 ± 6.3 vs. 25.6 ± 7.6 μV, $p = 0.088$), duration (778.4 ± 41.1 vs. 794.2 ± 49.2 ms, $p = 0.385$), density (3.7 ± 0.8 vs. 4.0 ± 0.7/min, $p = 0.288$), or average frequency (11.9 ± 1.2 vs. 12.4 ± 0.9 Hz, $p = 0.287$) between iRBD patients and controls. However, the spindle power of iRBD patients was significantly lower than that of controls (0.67 ± 0.12 vs. 0.87 ± 0.18, $p = 0.002$; Table 3 and Supplementary

Table 2. Polysomnographic findings

Parameters	iRBD ($n = 16$)	Control ($n = 10$)	p
Total sleep time, min	396.2 ± 80.7	389.6 ± 73.6	0.586
Sleep latency, min	12.5 ± 16.5	7.2 ± 9.8	0.551
REM latency, min	87.0 ± 49.5	106.4 ± 79.4	0.586
WASO, min	62.6 ± 42.6	91.2 ± 50.8	0.097
Sleep efficiency, %	83.9 ± 11.9	79.7 ± 11.7	0.286
Stage N1, %	13.4 ± 5.9	14.4 ± 5.1	0.551
Stage N2, %	52.5 ± 7.5	48.6 ± 10.2	0.241
Stage N3, %	10.6 ± 8.0	17.1 ± 10.0	0.121
Stage R, %	23.5 ± 5.0	19.9 ± 6.2	0.165
AHI, /h	6.1 ± 3.5	10.2 ± 3.9	0.009
Arousal index, /h	13.2 ± 6.2	18.3 ± 6.1	0.077
RSWA			
Tonic, %	39.7 ± 21.0	4.1 ± 3.6	<0.001*
Phasic, %	11.9 ± 10.3	1.4 ± 1.4	0.001*

Data are presented as mean ± standard deviation. Wilcoxon rank-sum tests were used compare the two groups. iRBD, idiopathic REM sleep behavior disorder; REM, rapid eye movement; WASO, wakefulness after sleep onset; AHI, apnea–hypopnea index; RSWA, REM sleep without atonia.
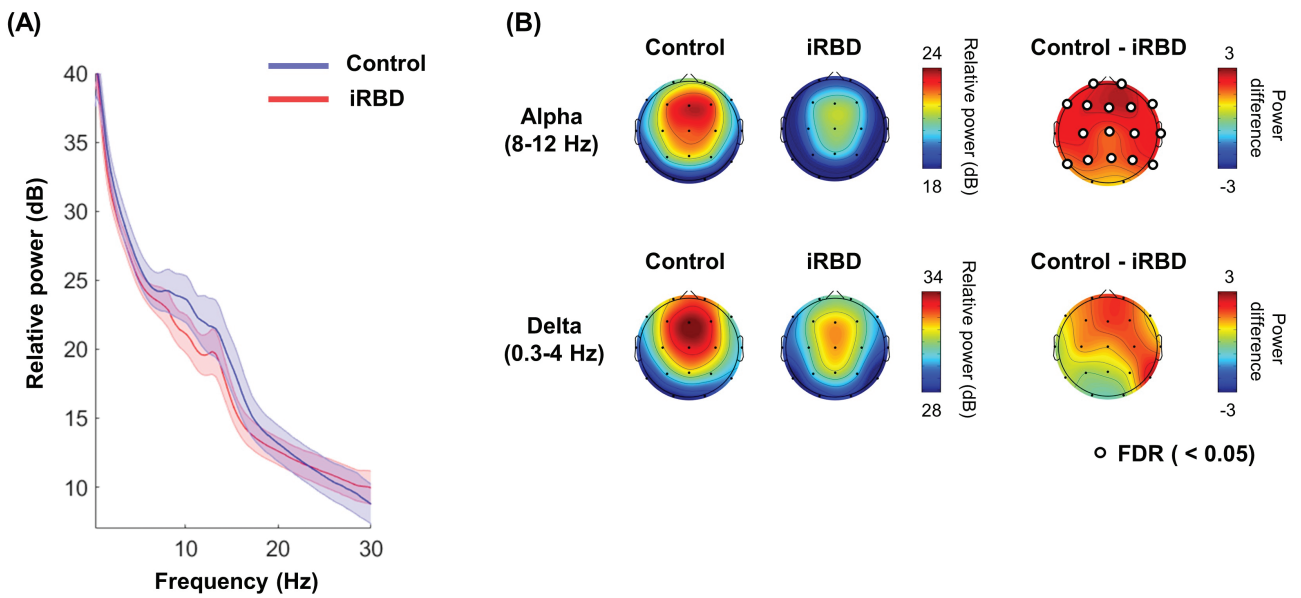*Significant after the Bonferroni correction ($\alpha = 0.05/13$).

Figure 1. EEG power spectral analysis during NREM sleep. (A) Averaged power spectrum at the frontal, central, and parietal regions (F3, Fz, F4, C3, Cz, C4, P3, Pz, and P4). There was no significant difference between the two groups after the Bonferroni correction for the frequency bands ($\alpha = 0.05/4$). Shading indicates the 95% confidence interval. (B) Scalp topography of alpha- and delta-band activities. White dots indicate electrodes showing a significant intergroup difference (FDR-corrected $p < 0.05$).
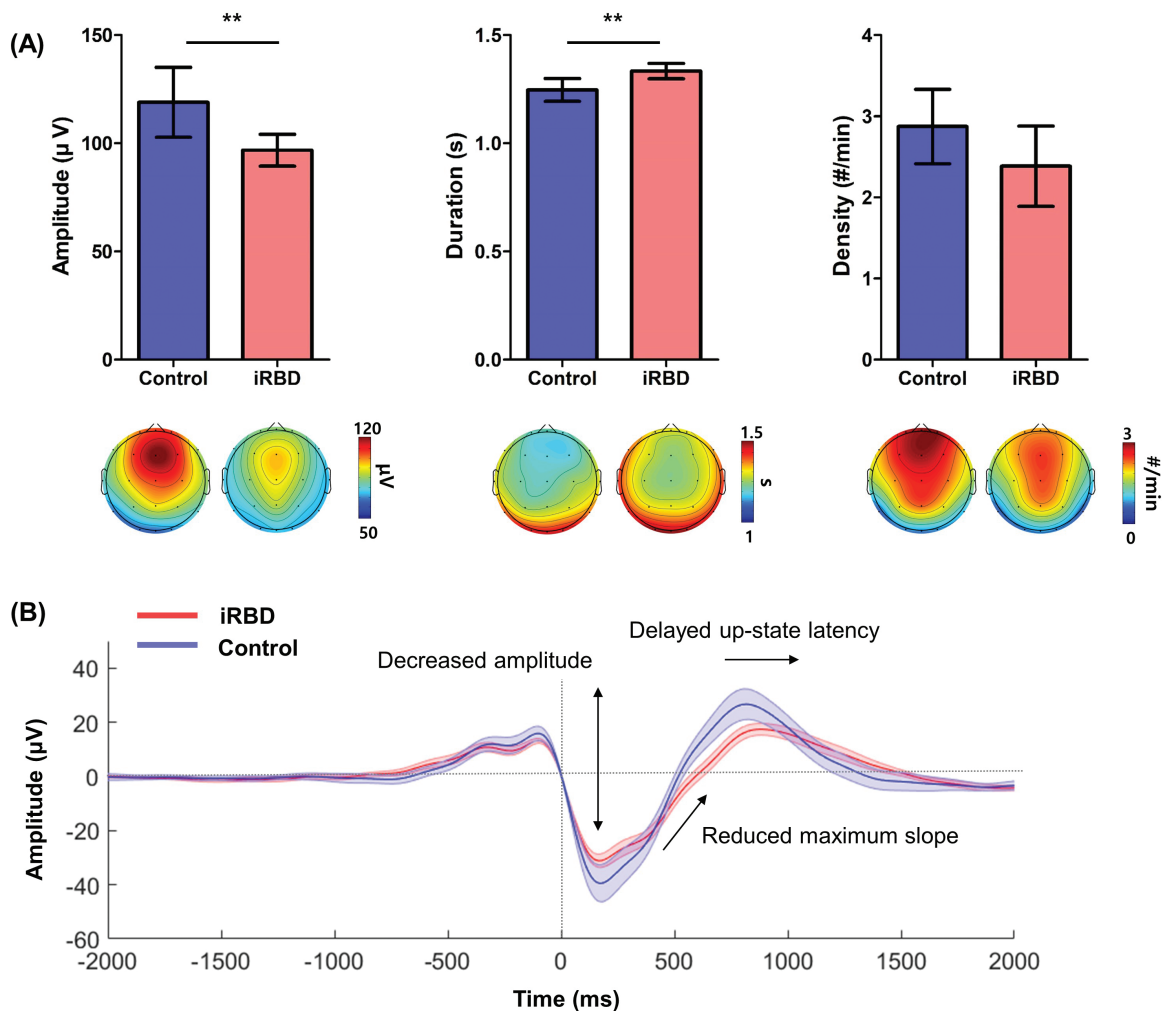

Figure 2. Comparison of SO characteristics. (A) SO amplitude, duration, and density measured at the frontal regions (F3, Fz, and F4; upper panel) and the corresponding scalp topography (lower panel). Error bars indicate the 95% confidence interval. Independent samples *t*-test, *$p < 0.05$, **$p < 0.01$. (B) Grand-averaged SO waveforms. A vertical line at 0 ms indicates the SO onset. Shading indicates the 95% confidence interval.

Table S1). Although the scalp topography of spindle power showed a centro-parietal maximum, the intergroup differences in spindle power were significant across the whole brain, with a maximum difference in the frontal region (Figure 3).

SO–SS coordination

Of the total SOs detected during NREM sleep, 16.2% in the iRBD group and 16.7% in the control group co-occurred with SS, and the ratio of SO-locked spindle density to total SO density did not differ between the two groups (p = 0.783). The SO-locked

Table 3. Results of SO and SS analysis

Variables	iRBD (n = 16)	Control (n = 10)	p
Slow oscillation			
Amplitude, μV	96.8 ± 13.8	118.9 ± 22.6	0.005*
Duration, s	1.33 ± 0.07	1.25 ± 0.07	0.005*
Density, /min	2.4 ± 0.9	2.9 ± 0.6	0.157
Maximum slope, μV/s	414.2 ± 51.6	535.7 ± 94.8	<0.001*
Up-state peak latency, ms	954.8 ± 61.8	865.4 ± 66.0	0.002*
Sleep spindle			
Amplitude, μV	20.8 ± 6.3	25.6 ± 7.6	0.088
Duration, ms	778.4 ± 41.1	794.2 ± 49.2	0.385
Density, /min	3.7 ± 0.8	4.0 ± 0.7	0.288
Average frequency, Hz	11.9 ± 1.2	12.4 ± 0.9	0.287
Power (log10)	0.67 ± 0.12	0.87 ± 0.18	0.002*
SO-locked spindle			
Density, /min	0.36 ± 0.13	0.47 ± 0.15	0.069
Power	0.95 ± 0.31	1.17 ± 0.49	0.167
Phase, rad	−0.51 ± 0.45	−0.04 ± 0.31	0.009*
Phase locking value	0.63 ± 0.06	0.64 ± 0.05	0.472

SO, slow oscillation.
*Significant after the Bonferroni correction (α = 0.05/5 for SO and SS; α = 0.05/4 for SO-locked spindle).

spindle density did not significantly differ between the groups (0.36 ± 0.13 vs. 0.47 ± 0.15/min, p = 0.069). Time-frequency maps showed that the SO-locked spindles occurred in the vicinity of the up-state peak of SOs in both groups (Figure 4, A). Although the SO-locked spindle power of iRBD patients seemed to be lower than that of controls, it was not statistically significant (0.95 ± 0.31 vs. 1.17 ± 0.49, p = 0.167). Thereafter, we evaluated the phase distribution of SO-locked SS with reference to the up-state peak of SOs. Compared with controls, patients with iRBD showed significant phase advances of SO-locked spindle activities (−0.51 ± 0.45 vs. −0.04 ± 0.31 rad, p = 0.009; Figure 4B; Table 3). In other words, SO-locked spindles of iRBD patients occurred during the down-to-up-state transition of SOs, whereas those of controls occurred during the up-state peak of SOs. However, after adjusting for age and other clinical variables, differences in the phase of SO-locked spindles failed to survive the Bonferroni correction (Supplementary Table S1). There was no significant difference in the PLV of SO-locked SS between the two groups (0.63 ± 0.06 vs. 0.64 ± 0.05, p = 0.472).

In the correlation analyses, the phase of SO-locked SS showed a significant positive correlation with the MoCA-K delayed recall subscores (r = 0.538, p = 0.005; Figure 5 and Table 4), suggesting that the phase advance of SO-locked spindles is associated with cognitive impairment. However, the phase of SO-locked SSs was not correlated with tonic (r = −0.364, p = 0.068) or phasic (r = −0.128, p = 0.533) EMG activity.

Discussion

In this study, we found significant alterations in SO and SS activities during NREM sleep in patients with iRBD. The SOs of iRBD patients had smaller and shallower morphology than those of controls. The SS power in patients with iRBD was decreased compared with that in controls. Moreover, the
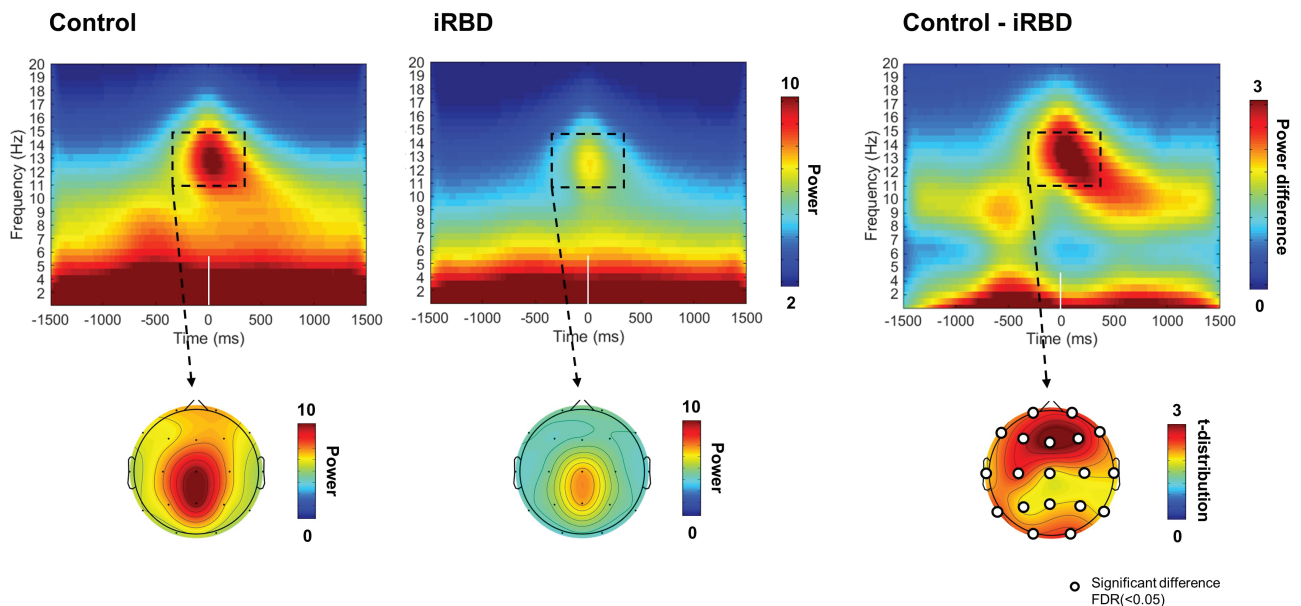
Figure 3. SS power in patients with iRBD and controls. The upper panel shows averaged time-frequency maps at frontal, central, and parietal regions (F3, Fz, F4, C3, Cz, C4, P3, Pz, and P4). The peak of the spindle envelope was aligned at 0 ms. Dotted boxes indicate the frequency (12–16 Hz) and time (from −400 to 400 ms) range of SSs. The corresponding topography maps of spindle power are depicted in the lower panel. White dots indicate electrodes showing a significant intergroup difference (FDR-corrected p < 0.05).
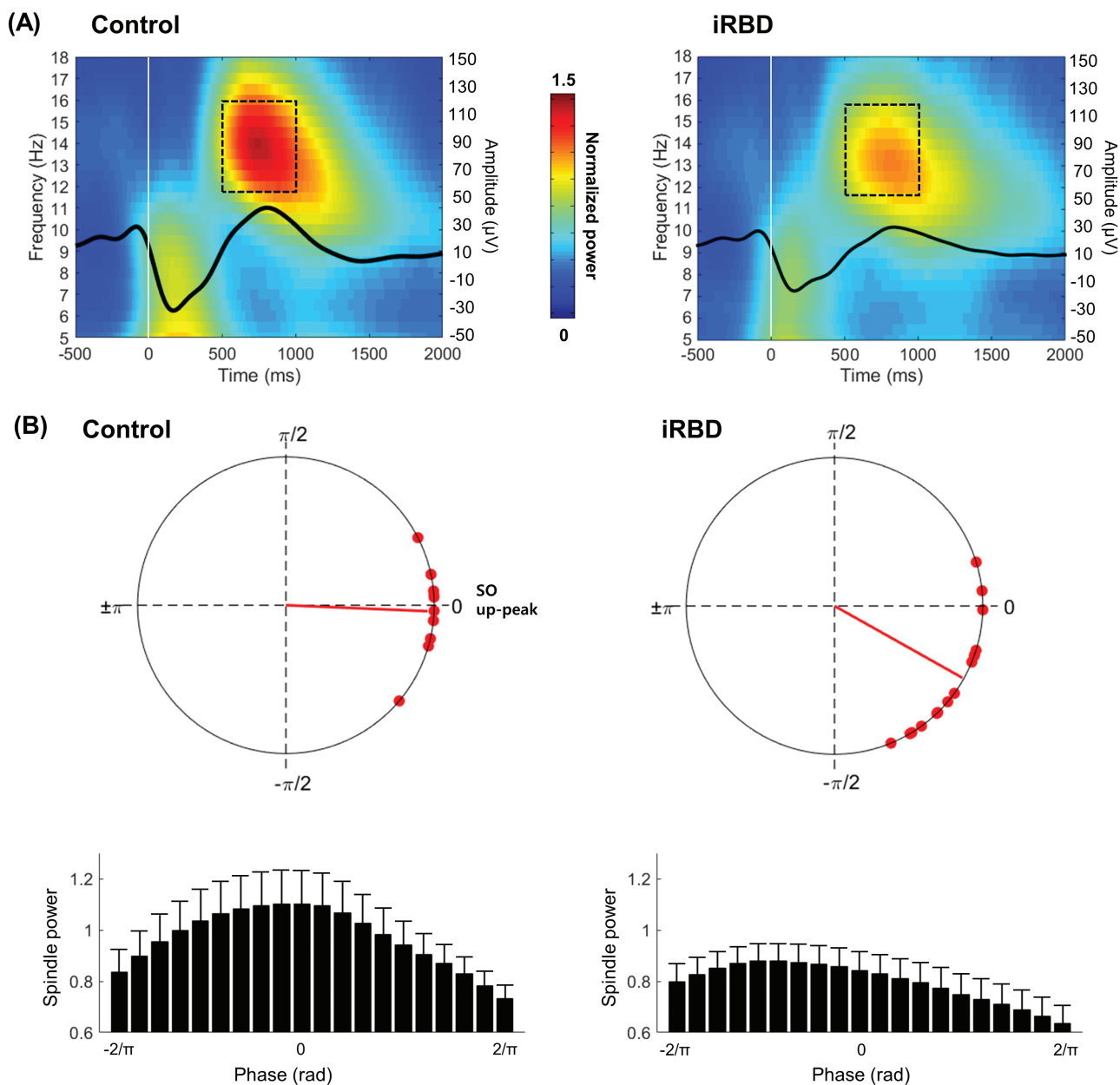
Figure 4. SO-locked SSs. (A) Averaged SO waveforms and time-frequency maps at frontal, central, and parietal regions (F3, Fz, F4, C3, Cz, C4, P3, Pz, and P4). Dotted boxes indicate the frequency (12–16 Hz) and time (from 500 to 1,000 ms) range where the SO-locked spindle power was measured. A vertical line at 0 ms indicates the SO onset. (B) Distribution of phase of SO-locked SSs with reference to the SO up-state peak (upper panel). Red lines indicate the averaged phase within each group. The lower panel shows distribution of normalized power of SO-locked spindles according to the phase. The phase of 0 rad indicates the up-state peak of SOs.

phase of SO-locked SSs was significantly advanced in patients with iRBD compared with that in controls, which was correlated with memory decline. It is noteworthy that the EEG signatures of NREM sleep were altered in patients with iRBD, even though iRBD is a REM sleep-related parasomnia caused by neurodegenerative loss of the REM atonia circuitry [29]. Although EEG slowing during both wakefulness and REM sleep has been reported in patients with iRBD, little evidence exists regarding EEG abnormalities during NREM sleep [30, 31]. Latreille et al. found no significant difference in delta power and slow wave characteristics during NREM sleep between the iRBD and control groups [32]. As opposed to the hypothesis that neural substrates responsible for NREM sleep are

unaffected in iRBD, our results demonstrated that the NREM sleep-specific brain oscillations, including SO and SS, were disrupted in iRBD.

SOs are one of the most important EEG signatures of NREM sleep and are known to synchronize neuronal activities into hyperpolarized down-states and depolarized up-states [2]. They originate from neocortical networks and provide a framework for communication between the neocortex and subcortical structures, which is implicated in memory consolidation during sleep [33]. In agreement with this, enhancing SOs during NREM sleep improved the consolidation of hippocampal-dependent declarative memory [34, 35]. The smaller and shallower morphology of SOs in iRBD patients coincides with age-related changes
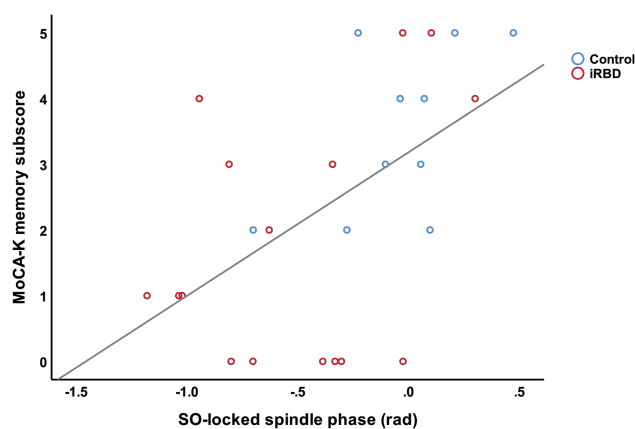
Figure 5. Correlation between the phase of SO-locked SSs and delayed recall subscore. MoCA-K, the Korean version of the Montreal Cognitive Assessment (MoCA-K); *r*, the Pearson correlation coefficient.

Table 4. Results of correlation analysis with the SO-locked spindle phase

Variables	*r*	*p*
MoCA-K score		
Total	0.440	0.025
Visuospatial/executive	−0.067	0.744
Naming	0.239	0.240
Attention	−0.103	0.616
Language	0.280	0.165
Abstraction	0.162	0.429
Delayed recall	0.538	0.005*
Orientation†	N/A	N/A
RSWA		
Tonic, %	−0.346	0.068
Phasic, %	−0.128	0.533

r indicates the Pearson correlation coefficient. MoCA-K, Korean version of Montreal cognitive assessment; RSWA, REM sleep without atonia.
*Significant after the Bonferroni correction (α = 0.05/9).
†Not available because all participants received the highest orientation subscore of 6.

in the slow-wave morphology [36]. Among the slow-wave morphology characteristics, decreased steepness tended to be associated with age-related cognitive decline. It is consistent with our findings that the decreased slope was the most significant difference in SO characteristics between iRBD patients and controls. A previous diffusion tensor imaging study showed that a steeper rising slope of SOs was associated with higher axial diffusivity in the frontal white matter tracts [37]. In this regard, the decreased slope of SOs in patients with iRBD may reflect a decline in axonal integrity and decreased cortical connectivity. Despite the abnormal morphology, the preserved SO density in patients with iRBD suggests that the cortical dysfunction was too modest to disrupt the SO generation per se, as shown in a study of first degree relatives of patients with schizophrenia [38].

In the present study, although there was no significant between-group difference in SS density, patients with iRBD had significantly decreased SS power compared with that of controls. In agreement with our findings, alterations in SS activity have been implicated in patients with iRBD and PD [18]. Decreased spindle density, amplitude, and average frequency at baseline was associated with the development of dementia in patients

with PD [6]. Moreover, patients with iRBD showed a reduced SS density, especially for fast spindles, compared with that of controls [19]. Preservation of SS density suggests that dysfunction of the thalamic spindle generator is not the primary cause of decreased spindle power in patients with iRBD. A more plausible explanation is the impaired transfer of thalamic spindles to the cortex and decreased cortical firing driven by thalamic spindles. In addition, small sample size, short disease duration, and lack of separate analysis for fast and slow spindles are also possible explanations for preserved SS density of iRBD patients in the present study.

An intracranial EEG study demonstrated that cortical spindles are generated in coordination with SOs by the cortico-thalamo-cortical pathway [39]. Therefore, the temporal coupling between SO and SS represents the integrity of thalamo-cortical networks. A previous study reported abnormal surface contraction in the bilateral thalamus and widespread cortical thinning in iRBD patients with mild cognitive impairment [16]. This supports the notion that patients with iRBD had impaired cortico-thalamic connection resulting in the abnormal coupling between SOs and SSs during NREM sleep. In the current study, SSs in patients with iRBD prematurely peaked during the down-to-up-state transition of SO, whereas SSs in controls were aligned with the SO up-state peak. This pattern of SO-spindle misalignment in iRBD patients is consistent with that seen in older adults relative to young adults [40], suggesting an accelerated aging or degenerative process in iRBD patients. The extent of phase advances of spindles from the SO up-state peak was correlated with the loss of memory retention. Furthermore, in a previous study showing a positive effect of zolpidem on overnight memory consolidation, zolpidem induced increased SS density and clustering of SSs closer to the SO up-state peak compared with placebo [41]. There was a positive correlation between SO-locked spindle phase and declarative memory performance, suggesting the importance of precise temporal coordination between SOs and SSs in memory consolidation during NREM sleep. This is in agreement with our results showing the correlation between the phase of SO-locked spindles and memory function in patients with iRBD. However, submentalis tonic and phasic EMG activity were not correlated with the phase of SO-locked SSs. Taken together, disruption of temporal coordination between SOs and SSs in iRBD patients may represent neurodegeneration involving the thalamo-cortical networks rather than the REM sleep atonia-generating brainstem circuit. It is also possible that abnormal SO morphology in patients with iRBD disturbed the temporal coordination between SOs and SSs.

There are several limitations in this study. The first is the small number of subjects studied. Especially, a smaller number of controls than iRBD patients might have led to bias or weakened statistical power. Because differences in the SO-locked spindle phase after adjusting for clinical variables did not survive the multiple testing correction, the possibility of false positive results should be considered when interpreting this data. Second, it cannot be concluded whether the abnormal SO and spindle activities are specific to neurodegenerative α-synucleinopathy. Further studies involving patients with PD and non-synucleinopathy diseases, such as Alzheimer's disease, are needed to address this issue. Third, because of the single-night vPSG protocol used in this study, a first night effect or night-to-night variability might have affected our data. Although the controls had no sleep complaints, 80%

(8/10) of them were found to have mild OSA. Fourth, we used algorithm-based automatic detectors for SS and SO. However, results of NREM sleep events can vary depending on different detection algorithms. Lastly, although the SO-spindle coordination reflects cortico-thalamo-cortical connections, scalp EEG is not able to determine neuronal activities in subcortical structures.

In summary, we found altered SO morphology, reduced spindle power, and abnormal SO-spindle coordination in patients with iRBD. These alterations in NREM sleep-specific EEG oscillations suggest that the disease processes of iRBD affect neuronal populations associated with not only REM sleep but also with NREM sleep. The impaired SO-spindle temporal coupling in iRBD may reflect early neurodegenerative changes involving the thalamo-cortical networks. Longitudinal studies are needed to determine that the NREM sleep EEG changes can predict the future development of neurodegeneration in patients with iRBD, especially in conjunction with other known iRBD biomarkers for future phenoconversion.

Supplementary Material

Supplementary material is available at *SLEEP* online.

Funding

References

1. Adamantidis AR, *et al*. Oscillating circuitries in the sleeping brain. *Nat Rev Neurosci*. 2019;**20**(12):746–762.
2. Steriade M, *et al*. A novel slow (< 1 Hz) oscillation of neocortical neurons in vivo: depolarizing and hyperpolarizing components. *J Neurosci*. 1993;**13**(8):3252–3265.
3. De Gennaro L, *et al*. Sleep spindles: an overview. *Sleep Med Rev*. 2003;**7**(5):423–440.
4. Castelnovo A, *et al*. Sleep spindles and slow waves in schizophrenia and related disorders: main findings, challenges and future perspectives. *Eur J Neurosci*. 2018;**48**(8):2738–2758.
5. Gorgoni M, *et al*. Parietal fast sleep spindle density decrease in Alzheimer's disease and amnesic mild cognitive impairment. *Neural Plast*. 2016;**2016**:8376108.
6. Latreille V, *et al*. Sleep spindles in Parkinson's disease may predict the development of dementia. *Neurobiol Aging*. 2015;**36**(2):1083–1090.
7. Mander BA, *et al*. Impaired prefrontal sleep spindle regulation of hippocampal-dependent learning in older adults. *Cereb Cortex*. 2014;**24**(12):3301–3309.
8. Mölle M, *et al*. Grouping of spindle activity during slow oscillations in human non-rapid eye movement sleep. *J Neurosci*. 2002;**22**(24):10941–10947.
9. Mölle M, *et al*. Fast and slow spindles during the sleep slow oscillation: disparate coalescence and engagement in memory processing. *Sleep*. 2011;**34**(10):1411–1421.
10. Schenck CH, *et al*. Chronic behavioral disorders of human REM sleep: a new category of parasomnia. *Sleep*. 1986;**9**(2):293–308.
11. Högl B, *et al*. Idiopathic REM sleep behaviour disorder and neurodegeneration—an update. *Nat Rev Neurol*. 2018;**14**(1):40–55.
12. Heinzel S, *et al*. Update of the MDS research criteria for prodromal Parkinson's disease. *Mov Disord*. 2019;**34**(10):1464–1470.
13. Postuma RB, *et al*. Risk and predictors of dementia and parkinsonism in idiopathic REM sleep behaviour disorder: a multicentre study. *Brain*. 2019;**142**(3):744–759.
14. Sunwoo JS, *et al*. Altered functional connectivity in idiopathic rapid eye movement sleep behavior disorder: a resting-state EEG Study. *Sleep*. 2017;**40**(6). doi:10.1093/sleep/zsx058
15. Byun J-I, *et al*. Altered resting-state thalamo-occipital functional connectivity is associated with cognition in isolated rapid eye movement sleep behavior disorder. *Sleep Med*. 2020;**69**:198–203.
16. Rahayel S, *et al*. Cortical and subcortical gray matter bases of cognitive deficits in REM sleep behavior disorder. *Neurology*. 2018;**90**(20):e1759–e1770.
17. Campabadal A, *et al*. Cortical gray matter and hippocampal atrophy in idiopathic rapid eye movement sleep behavior disorder. *Front Neurol*. 2019;**10**:312.
18. Christensen JA, *et al*. Decreased sleep spindle density in patients with idiopathic REM sleep behavior disorder and patients with Parkinson's disease. *Clin Neurophysiol*. 2014;**125**(3):512–519.
19. O'Reilly C, *et al*. REM sleep behaviour disorder is associated with lower fast and higher slow sleep spindle densities. *J Sleep Res*. 2015;**24**(6):593–601.
20. Schreiner SJ, *et al*. Slow-wave sleep and motor progression in Parkinson disease. *Ann Neurol*. 2019;**85**(5):765–770.
21. Massimini M, *et al*. The sleep slow oscillation as a traveling wave. *J Neurosci*. 2004;**24**(31):6862–6870.
22. American Academy of Sleep Medicine. *International Classification of Sleep Disorders*. 3rd ed. Darien, IL: American Academy of Sleep Medicine; 2014.
23. Berry RB, *et al*. *The AASM Manual for the Scoring of Sleep and Associated Events: Rules, Terminology and Technical Specifications, Version 2.2*. Darien, IL: American Academy of Sleep Medicine; 2015.
24. McCarter SJ, *et al*. Submentalis rapid eye movement sleep muscle activity: a potential biomarker for synucleinopathy. *Ann Neurol*. 2019;**86**(6):969–974.
25. Weber FD. SpiSOP software repository, SpiSOP—Spindles, slow oscillations, power density and fast replication of basic sleep EEG analyses in one tool. 2019. https://www.spisop.org. Accessed October 2019.
26. Cha KS, *et al*. Impaired slow oscillation, sleep spindle, and slow oscillation-spindle coordination in patients with idiopathic restless legs syndrome. *Sleep Med*. 2020;**66**:139–147.
27. Muehlroth BE, *et al*. Understanding the interplay of sleep and aging: methodological challenges. *Psychophysiology*. 2020;**57**(3):e13523.
28. Lachaux JP, *et al*. Measuring phase synchrony in brain signals. *Hum Brain Mapp*. 1999;**8**(4):194–208.
29. Luppi PH, *et al*. The neuronal network responsible for paradoxical sleep and its dysfunctions causing narcolepsy and rapid eye movement (REM) behavior disorder. *Sleep Med Rev*. 2011;**15**(3):153–163.
30. Sasai T, *et al*. Electroencephalographic findings related with mild cognitive impairment in idiopathic rapid eye movement sleep behavior disorder. *Sleep*. 2013;**36**(12):1893–1899.

31. Rodrigues Brazète J, *et al*. Electroencephalogram slowing in rapid eye movement sleep behavior disorder is associated with mild cognitive impairment. *Sleep Med.* 2013;**14**(11):1059–1063.

32. Latreille V, *et al*. Non-rapid eye movement sleep characteristics in idiopathic REM sleep behavior disorder. *J Neurol Sci.* 2011;**310**(1–2):159–162.

33. Diekelmann S, *et al*. The memory function of sleep. *Nat Rev Neurosci.* 2010;**11**(2):114–126.

34. Marshall L, *et al*. Boosting slow oscillations during sleep potentiates memory. *Nature.* 2006;**444**(7119):610–613.

35. Ngo HV, *et al*. Auditory closed-loop stimulation of the sleep slow oscillation enhances memory. *Neuron.* 2013;**78**(3):545–553.

36. Ujma PP, *et al*. Individual slow-wave morphology is a marker of aging. *Neurobiol Aging.* 2019;**80**:71–82.

37. Piantoni G, *et al*. Individual differences in white matter diffusion affect sleep oscillations. *J Neurosci.* 2013;**33**(1):227–233.

38. D'Agostino A, *et al*. Sleep endophenotypes of schizophrenia: slow waves and sleep spindles in unaffected first-degree relatives. *NPJ Schizophr.* 2018;**4**(1):2.

39. Mak-McCully RA, *et al*. Coordination of cortical and thalamic activity during non-REM sleep in humans. *Nat Commun.* 2017;**8**:15499.

40. Helfrich RF, *et al*. Old brains come uncoupled in sleep: slow wave-spindle synchrony, brain atrophy, and forgetting. *Neuron.* 2018;**97**(1):221–230.e4.

41. Zhang J, *et al*. The effect of zolpidem on memory consolidation over a night of sleep. *Sleep.* 2020. doi:10.1093/sleep/zsaa084